Hexokinase 2 from *Saccharomyces cerevisiae:* Regulation of Oligomeric Structure by *in Vivo* Phosphorylation at Serine-14†

Joachim Behlke,‡ Katja Heidrich,§ Manfred Naumann,|| Eva-Christina Müller,‡ Albrecht Otto,‡ Renate Reuter,|| and Thomas Kriegel*,§

Medizinische Fakultät Carl Gustav Carus, Institut für Physiologische Chemie, Technische Universität Dresden, Karl-Marx-Strasse 3, D-01109 Dresden, Germany, Max-Delbrück-Centrum für Molekulare Medizin, D-13122 Berlin, Germany, and Medizinische Fakultät, Institut für Biochemie, Universität Leipzig, Liebigstrasse 16, D-04103 Leipzig, Germany

Received April 22, 1998; Revised Manuscript Received June 25, 1998

ABSTRACT: Homodimeric hexokinase 2 from *Saccharomyces cerevisiae* is known to have two sites of phosphorylation: for serine-14 the modification *in vivo* increases with glucose exhaustion [Kriegel et al. (1994) *Biochemistry 33,* 148−152], while for serine-157 it occurs *in vitro* with ATP in the presence of nonphosphorylateable five-carbon analogues of glucose [Heidrich et al. (1997) *Biochemistry 36,* 1960−1964]. We show now by site-directed mutagenesis and sedimentation analysis that serine-14 phosphorylation affects the oligomeric state of hexokinase, its substitution by glutamate causing complete dissociation; glutamate exchange for serine-157 does not. Phosphorylation of wild-type hexokinase at serine-14 likewise causes dissociation *in vitro*. In view of the higher glucose affinity of monomeric hexokinase and the high hexokinase concentration in yeast [Womack, F., and Colowick, S. P. (1978) *Arch. Biochem. Biophys. 191,* 742−747; Mayes, E. L., Hoggett, J. G., and Kellett, G. L. (1983) *Eur. J. Biochem. 133,* 127−134], we speculate that the *in vivo* phosphorylation at serine-14 as transiently occurring in glucose derepression might provide a mechanism to improve glucose utilization from low level and/or that nuclear localization of the monomer might be involved in the signal transduction whereby glucose causes catabolite repression.

Hexokinase 2[1] (gene name *HXK2*) is the predominating hexose kinase in *Saccharomyces cerevisiae* in growth on glucose (*1, 2*) and is also required for catabolite repression by glucose of expression of other genes (e.g., *3*−*7*). Two other isoenzymes, hexokinase 1 (gene *HXK1*) and glucokinase (gene *GLK1*), are also singly adequate for growth on glucose, but their normal expression is highest on other carbon sources (*2, 8, 9*).

Hexokinase 2 exists in solution at neutral pH as a dimeric protein with a molecular mass of approximately 104 kDa (*10*). Increasing pH or ionic strength leads to its partial dissociation into identical monomers (*11*−*13*). While glucose alone exerts a weak dissociative effect, the synergistic action of this substrate with the reaction product MgADP causes substantial enzyme dissociation (*10, 13*). The identification of the catalytically active hexokinase species predominating *in vivo* is still a matter of debate. Sedimentation analysis specifically detecting catalytically active hexokinase (active enzyme centrifugation) revealed a stabilization of the dimeric species by the simultaneous presence of both substrates (*14*), whereas studies employing reacting enzyme gel filtration showed that monomeric hexokinase was predominant in conditions of *in vitro* catalysis (*15*). Estimations of the average intracellular concentration of hexokinase would predict that the enzyme might normally be a homodimer *in vivo* (*16*). The finding that short forms (S-forms) of hexokinase created *in vitro* by limited proteolysis (*17, 18*) or by truncation employing genetic deletion (*19*) of the N-terminus, respectively, are monomers *in vitro* indicates a decisive role of this region for intersubunit interaction.

The yeast hexokinases are known to exist as phosphoproteins *in vivo* (*20*). In a condition of glucose depletion, phosphorylation increases at serine-14. This site belongs to one of two sequence motifs (amino acids 11−14 and 381−384) resembling protein kinase A targets, and serine-14 is also specifically phosphorylated by protein kinase A *in vitro* (*21*). In the presence of ATP and nonphosphorylatable five-carbon analogues of glucose, hexokinase *in vitro* undergoes autophosphorylation−inactivation (*22*) at serine-157 (*23*). This latter residue is known to be involved in substrate binding (*24*), its enzymatic dephosphorylation restores hexokinase activity (*23*). Neither the function of *in vivo* phosphorylation at serine-14 nor the enzyme(s) involved are known. Likewise, although D-xylose can stimulate inactivation of hexokinase 2 *in vivo* (*25*), it is not known whether the serine-157 modification occurs in a normal physiological situation.

† Supported by DFG Grant Kr 1162/3-1 (T.K.). This work was initiated with Dan G. Fraenkel in the Department of Microbiology and Molecular Genetics at Harvard Medical School with the support of NIH Grant GM 21098.

* To whom correspondence should be addressed. Phone: (49)-(351)8832871. Fax: (49)(351)8832869. E-mail: kriegel@rcs.urz.tu-dresden.de.

‡ Max-Delbrück-Centrum für Molekulare Medizin.

§ Technische Universität Dresden.

|| Universität Leipzig.

[1] Enzyme: hexokinase, ATP:D-hexose 6-phosphotransferase (EC 2.7.1.1).

S0006-2960(98)00914-3 CCC: $15.00 © 1998 American Chemical Society
Published on Web 08/07/1998

To evaluate the structural and functional consequences of hexokinase interconversion by phosphorylation−dephosphorylation, mutant forms of the enzyme obtained by amino acid substitution for serine-14 and serine-157, respectively, were studied by two methods of sedimentation analysis. While substitution of alanine, cysteine, and glutamate, respectively, for serine-157 was found not to affect the association−dissociation equilibrium of hexokinase, both permanent pseudophosphorylation by serine−glutamate exchange at serine-14 and *in vivo* phosphorylation itself are shown to change the conformation and oligomeric structure of this enzyme.

EXPERIMENTAL PROCEDURES

Strains, Plasmids, Site-Directed Mutagenesis, Enzyme Purification. The triple kinase mutant strain DFY632 (*hxk1::LEU2 hxk2::LEU2 glk1::LEU2 lys1-1 leu2-1 ura3-52*) of *Saccharomyces cerevisiae* (*20*) was used for the expression and isolation of wild-type and mutant hexokinases. The construction of hexokinase 2 mutations at serine-14 and serine-157 and the preparation of the different forms of the enzyme are described elsewhere (*21, 23*); glutamate-14 hexokinase was obtained employing the same strategy. Phosphoserine-14 hexokinase was separated from the non-phosphorylated wild-type enzyme by substituting hydroxylapatite adsorption (*21*) for DEAE rechromatography (*23*). Alternatively, phosphoserine-14 hexokinase was isolated from cells grown in full-phosphate medium omitting phosphate depletion as originally described (*20*).

Enzyme Assay (Standard Conditions). Hexokinase activity was determined spectrophotometrically in 50 mM triethanolamine hydrochloride buffer containing 5.0 mM glucose, 10 mM $MgCl_2$, 1.0 mM ATP, and 0.5 mM $NADP^+$ at pH 7.4 and 25 °C with glucose-6-phosphate dehydrogenase as auxiliary enzyme.

Molar UV Absorption Coefficients and Partial Specific Volume of Hexokinase. The enzyme was dialyzed exhaustively against bidistilled water. Aliquots of the dialyzed protein were either used to scan its UV absorbance spectrum or subjected to hydrolysis followed by determination of the amino acid composition according to (*26*). The data obtained are given in Table 1. The partial specific volume, $\bar{v}$, of hexokinase was calculated from the amino acid composition (*27, 28*) and the density increment of the individual amino acids (*29*).

Analytical Ultracentrifugation. Molecular mass studies were carried out in an XL-A-type analytical ultracentrifuge (Beckman) equipped with UV absorbance scanner optics. Two different methodical variants were employed; (i) sedimentation equilibrium analysis to directly determine the molecular mass; and (ii) velocity sedimentation to obtain additional hydrodynamic parameters (sedimentation and diffusion coefficients). Sedimentation equilibrium was analyzed using externally loaded six-channel centerpieces of 12 mm optical path usually filled with 100 μL of liquid. This type of cell allows the analysis of three solvent−solution pairs (*30*). Three or seven of these cells were used to simultaneously analyze different samples in one and the same run. Sedimentation equilibrium was reached after 2 h of overspeed at 16 000 rpm, followed by an equilibrium speed of 12 000 rpm at 10 °C for 24−30 h (*31*). The radial absorbancies of each compartment were scanned at three different wavelengths, routinely at 280, 285, and 290 nm, using the molar absorption coefficients determined with wild-type hexokinase (this paper).

Molecular mass calculations were done by simultaneously fitting the sets of three radial absorbance distribution curves being described by eq 1

$$A_r = A_{r,m} \exp[MK(r^2 - r_m^2)] \quad (1)$$

with

$$K = [(1 - \rho\bar{v})\omega^2]/2RT \quad (2)$$

using our computer program Polymole (*32*). In this equation, ρ is the solvent density, $\bar{v}$ is the partial specific volume, ω is the angular velocity, R is the gas constant, and T is the absolute temperature. A_r is the radial absorbance, and $A_{r,m}$ is the corresponding value at the meniscus position. The program Polymole also allows the analysis of self-associating proteins including a determination of partial concentrations and association constants which are derived from the best fit of the radial concentration distribution data. For yeast hexokinase known to represent a structurally closed system comprising monomeric and dimeric species only, the experimental data were correspondingly examined for a monomer−dimer equilibrium.

Sedimentation velocity experiments were done in standard double sector cells filled with 300 μL of solution at 26 000 rpm and 20 °C. From the time-dependent radial concentration profiles alternatively recorded at either 280 or 285 nm, sedimentation and diffusion coefficients were simultaneously determined employing the Lamm program (*33*). The combination of both parameters with the partial specific volume as determined from the amino acid composition of wild-type hexokinase allows to calculate the molecular mass, M_{sD}, using the Svedberg equation. Furthermore, the frictional ratio f/f_0 was calculated from these parameters using eq 3.

$$f/f_0 = 10^{-8}\left(\frac{1 - \rho\bar{v}}{sD^2\bar{v}}\right)^{1/3} \quad (3)$$

This complex parameter consists of a shape-dependent and a hydration-dependent component. Assuming an average hydration of 0.30 g of H_2O per gram of protein (*34*), the gross conformation of a protein in solution can be estimated from the remaining value in eq 3 representing the shape-dependent component of f/f_0.

Tryptic Digestion, Peptide Mapping, N-Terminal Sequencing, Mass Spectrometry. Hexokinase was bound to Poros 20 R1 reverse-phase material (PerSeptive Biosystems), washed with 0.1% trifluoroacetic acid, and eluted with 60% acetonitrile containing 0.1% trifluoroacetic acid. Volumes containing 200 pmol of protein were taken to dryness in a Speedvac centrifuge and were digested at 36 °C for 15 h with 0.5 mg of sequencing-grade modified trypsin (Promega) dissolved in 0.1 M Tris/HCl buffer, pH 8.1. Tryptic peptide maps were obtained by reverse-phase HPLC (μRPC C2/C18 SC 2.1/10 column/Smart system; Pharmacia Biotech) at 26 °C employing a gradient of acetonitrile in 0.1% trifluoroacetic acid. For Edman degradation, the different forms of native and mutant hexokinase as well as peptides of interest from tryptic digests of the enzyme were loaded onto a

Biobrene-coated glass filter fiber of a Procise sequencer (Applied Biosystems) and were sequenced using standard protocols.

Mass spectrometry (MS) and tandem mass spectrometry (MS/MS) were performed on a nanoelectrospray ionization hybrid quadrupole−orthogonal acceleration time-of-flight Q-Tof instrument (Micromass UK Ltd.) equipped with a Z-spray probe. The nanoflow source was operated at a temperature of 30 °C with a nitrogen drying gas flow of 180 L/h. A potential of 1.4 kV was applied to the nanoflow tip. The flow rate was about 30 nL/min. Peptides were dissolved in 5 μL of methanol/water (50% v/v) containing 1% formic acid. Aliquots of 1 μL, respectively, were required for a single measurement.

Chemicals, Molecular Biology Reagents, Enzymes. Media constituents were from Difco. Restriction enzymes and buffers were obtained from Boehringer. Mutagenizing PCR was done on a Gene ATAQ Controller (Pharmacia Biotech) employing the Expand High Fidelity System (Boehringer).

5′-Phosphorylated oligonucleotides were custom-made by Perkin-Elmer. PCR products were purified using the QIAquick PCR Purification Kit (Qiagen). The Blunting End Ligation Set was an MBI Fermentas product. DNA was isolated from agarose gels by use of the QIAEX II Gel Extraction Kit (Qiagen). The Sequenase 2.0 DNA Sequencing Kit used was from U. S. Biochemicals. For automated sequencing, the Cy5 Auto Read Sequencing Kit (Pharmacia Biotech) was used. Hexokinase substrates, effectors, and auxiliary enzymes were from Boehringer and Sigma, respectively.

RESULTS

Enzyme Purification and Characterization. The isolation of the different forms of wild-type and mutant hexokinase described below from yeast strain DFY632/pAV101 and derivatives gives enzyme preparations of more than 95% purity with a minimum specific catalytic activity of 350 units/mg (standard assay) for the nonphosphorylated wild-type enzyme (cf. Table 4). Site-directed mutagenesis at codon positions 15 and 158 had been confirmed by automated sequencing of the *HXK2* ORF as well as by matrix-assisted laser desorption/ionization time-of-flight mass spectrometry and by sequencing of the isolated tryptic peptides (*23*). To investigate the structural and functional consequences of serine substitution/modification at the *in vivo* and autophosphorylation site, the intactness of the N-terminus known to be involved in intersubunit interaction (*17*−*19*) and the state of phosphorylation of serine-14 representing the target of *in vivo* phosphorylation (*21*) had to be checked since there is no information available on the long-term stability of hexokinase preparations with respect to proteolysis and phosphoserine hydrolysis.

With all hexokinase species employed in the present study, Edman degradation gave the N-terminal sequence: H-Val-His-Leu-Gly-Pro-Lys-Lys-Pro-Gln-Ala-Arg-Lys-Gly-Ser-Met-Ala-Asp-Val-OH, which corresponds to codons 2−19 of hexokinase according to the DNA primary structure (*27, 28*).[2] Hydroxylapatite fractionation of DEAE-purified wild-type hexokinase isolated from cells grown in low-glucose medium gave the two enzyme fractions (HA-1, HA-2) known to differ in the state of serine-14 modification only (*21*). These proteins were subjected to tryptic digestion followed by comparative HPLC reverse-phase analysis and peptide isolation as already described (*21*). Nanoelectrospray ionization mass spectrometry of the two peptides (spectra not shown) gave mass/charge ratios of 932.4 [$(M+H)^+$]/466.7 [$(M+2H)^{2+}$] and 1012.9 [$(M+H)^+$]/506.9 [$(M+2H)^{2+}$] which agree with the values calculated for the peptide carrying serine-14 unsubstituted (932.5) and phosphoserine-14 (1012.5), respectively. Conventional Edman degradation and tandem mass spectrometry (spectra not shown) confirmed the sequence H-Lys-Gly-Ser-Met-Ala-Asp-Val-Pro-Lys-OH for the unphosphorylated peptide which coincides with amino acids 12−20 of hexokinase (*27, 28*). Sequencing of the peptide obtained with phosphohexokinase gave the same order of residues but no signal in the third cycle of degradation corresponding to serine-14, thus indicating phosphorylation of this residue (*21*). MS/MS analysis of the latter peptide confirmed serine-14 phosphorylation (spectra not shown).

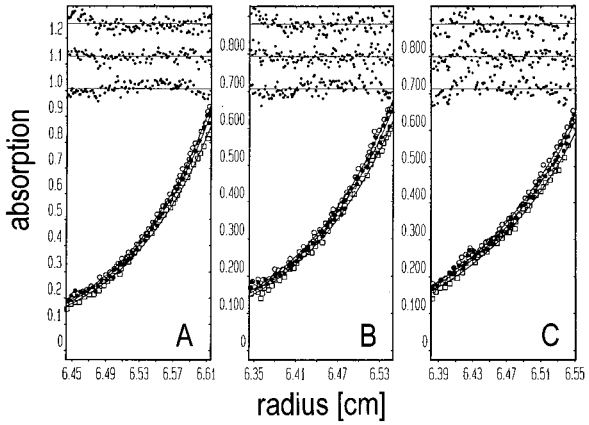

FIGURE 1: Sedimentation equilibrium distribution (symbols) and fitted data (curves) of yeast hexokinase 2 as recorded at 275 nm (●), 280 nm (○), and 285 nm (□). (A) Nonphosphorylated wild-type enzyme; (B) glutamate-14 hexokinase; (C) phosphoserine-14 enzyme. Solvent: 50 mM potassium phosphate buffer, pH 7.4, containing 1 mM PMSF, 1 mM EDTA, and 1 mM DTT. Loading enzyme concentration: 0.25−0.30 mg/mL. Temperature: 10 °C. Residuals (above) are given in 2-fold amplification.

Based on the results of DNA and protein analysis, the hydroxylapatite fractions HA-1 and HA-2 of purified hexokinase were considered to represent nonphosphorylated wild-type enzyme and phosphoserine-14 hexokinase, respectively.

It should be noted that *in vivo* phosphorylation of hexokinase 2 at serine-14 was detected not only in yeast grown in the phosphate-depleted medium (*20*), as originally employed to study protein phosphorylation, but also in cells from yeast extract peptone medium providing full availability of inorganic phosphate. Hydroxylapatite chromatography as well as tryptic peptide separation and analysis gave indistinguishable results with the enzymes prepared from cells grown in the two media differing in phosphate concentration.

Sedimentation Equilibrium Analysis. The molecular mass of wild-type hexokinase was determined from the radial concentration distributions shown in Figure 1A. These experiments covered a range of enzyme concentrations between 180 and 320 μg/mL as calculated directly from the

[2] Since the N-terminal amino acid of wild-type, mutant and phosphohexokinases corresponds to codon 2 of the ORF, we number amino acid residues accordingly (serine-14 instead of serine-15, etc.).

Table 1: Molar UV Absorption Coefficients of Wild-Type Yeast Hexokinase 2 As Determined by Spectrometry and Amino Acid Analysis[a]

wavelength (nm)	E (mM^{-1} cm^{-1})
275	48.12
280	49.83
285	45.60
290	31.62
295	18.87
300	9.55
305	6.25

[a] Molar concentrations are referred to monomeric hexokinase exhibiting a molecular mass of 53.948 Da (*27*, *28*).

Table 2: Molecular Mass of Different Forms of Wild-Type and Mutant Yeast Hexokinase 2 As Determined by Sedimentation Equilibrium Analysis

Hxk2 species	amino acid substitution/ modification	weight-average molecular mass, M_w (kDa)
Hxk2(S14/S157)[a]	none	103.1 ± 2.0
Hxk2(S14A/S157)	Ser-14 → Ala-14	87.6 ± 8.5
Hxk2(S14E/S157)	Ser-14 → Glu-14	53.4 ± 1.2
Hxk2(S14p/S157)	Ser-14 → phosphoser-14	53.5 ± 1.7
Hxk2(S14/S157A)	Ser-157 → Ala-157	103.5 ± 0.5
Hxk2(S14/S157C)	Ser-157 → Cys-157	105.7 ± 0.9
Hxk2(S14/S157E)	Ser-157 → Glu-157	102.6 ± 1.2

[a] Wild-type enzyme carrying serine-14 and serine-157 unsubstituted/unmodified.

UV scans using the absorption coefficients summarized in Table 1. The value of 103.1 ± 2.0 kDa (Table 2) indicates the enzyme to exist almost completely in the dimeric form. Amino acid exchanges at position 157 from serine to alanine, cysteine, and glutamate, respectively, gave similar results revealing the oligomeric structure of the enzyme to remain essentially unaffected (Table 2). In contrast, substitution/ modification of serine-14 resulted in significant changes in the hydrodynamic properties of hexokinase (Figure 1B,C; Tables 2 and 3). Alanine at this position was found to allow the formation of a well-balanced monomer−dimer equilibrium as illustrated in Figure 2. For this enzyme, the partial concentrations of monomer (M) and dimer (D), respectively, correspond to an association constant for dimerization of 1×10^6 M^{-1} which is lower by more than 1 order of magnitude than the value of 4×10^7 M^{-1} obtained for wild-type hexokinase (cf. Tables 2 and 3). The introduction of a negatively charged residue by serine−glutamate exchange caused a complete dissociation of hexokinase into its subunits as indicated by the lower slope of the radial concentration distribution curves (Figure 1B) corresponding to a molecular

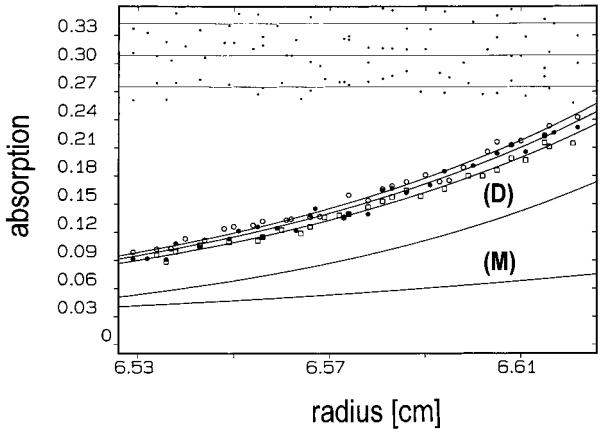

FIGURE 2: Radial concentration distribution of alanine-14 yeast hexokinase 2 at sedimentation equilibrium (conditions as in Figure 1). The primary data (symbols) were fitted to a monomer−dimer equilibrium and correspond to curves (M) and (D) describing the concentration distribution of monomeric and dimeric enzyme, respectively. From the partial concentrations of both molecular species determined by numerical integration of the areas below the curves, an association constant of $K_a = 1 \times 10^6$ M^{-1} was estimated. Residuals (above) are given in 2-fold amplification.

mass of 53.4 ± 1.2 kDa (Table 2). The latter enzyme constructed to mimic permanent phosphorylation as presumed to occur in conditions of glucose limitation should represent fully dissociated hexokinase. As anticipated, the same molecular mass of 53.5 ± 1.7 kDa and very similar changes of the molecular shape were found to result from the *in vivo* phosphorylation of hexokinase, demonstrating that serine-14 modification may completely transfer the enzyme into the monomeric state (Figure 1C; Tables 2 and 3).

Sedimentation−Diffusion Studies. Velocity sedimentation and on-line data analysis allowing the simultaneous determination of sedimentation and diffusion coefficients were performed to evaluate the hydrodynamic consequences of the individual amino acid exchanges at *in vivo* and autophosphorylation−inactivation site of hexokinase. This analytical technique is appropriate to derive from the primary sedimentation−diffusion data not only the molecular mass but also information about the gross conformation of the macromolecule. From the moving boundary (Figure 3) fitted by model functions of the Lamm program (*33*) sedimentation coefficients of 5.71 ± 0.03 S and diffusion coefficients of (5.37 ± 0.10) × 10^{-7} cm^2/s were derived for wild-type hexokinase (Figure 3A; Table 3). The use of these data and the introduction into the Svedberg equation of a partial specific volume $\bar{v} = 0.740$ mL/g as determined from amino acid analysis (cf. Experimental Procedures) result in a

Table 3: Sedimentation and Diffusion Coefficients, Molecular Mass, and Frictional Ratio of Different Forms of Wild-Type and Mutant Yeast Hexokinase 2 As Determined by Sedimentation Velocity Analysis

Hxk2 species	$s_{20,w}$ (S)	$D_{20,w}$ ($\times 10^{-7}$ cm^2/s)	M_{sD} (kDa)	f/f_0
Hxk2(S14/S157)[a]	5.71 ± 0.03	5.37 ± 0.10	99.7 ± 2.0	1.29 ± 0.02
Hxk2(S14A/S157)	4.77 ± 0.14	5.57 ± 0.33	80.3 ± 7.0	1.33 ± 0.06
Hxk2(S14E/S157)	3.99 ± 0.05	7.00 ± 0.10	53.4 ± 1.0	1.22 ± 0.02
Hxk2(S14p/S157)	4.00 ± 0.09	6.93 ± 0.12	54.1 ± 2.1	1.22 ± 0.02
Hxk2(S14/S157A)	5.57 ± 0.10	5.11 ± 0.27	102.3 ± 7.6	1.34 ± 0.05
Hxk2(S14/S157C)	5.59 ± 0.10	5.10 ± 0.24	102.7 ± 7.0	1.34 ± 0.04
Hxk2(S14/S157E)	5.80 ± 0.11	5.22 ± 0.26	104.1 ± 5.6	1.31 ± 0.03

[a] Wild-type enzyme carrying serine-14 and serine-157 unsubstituted/unmodified.

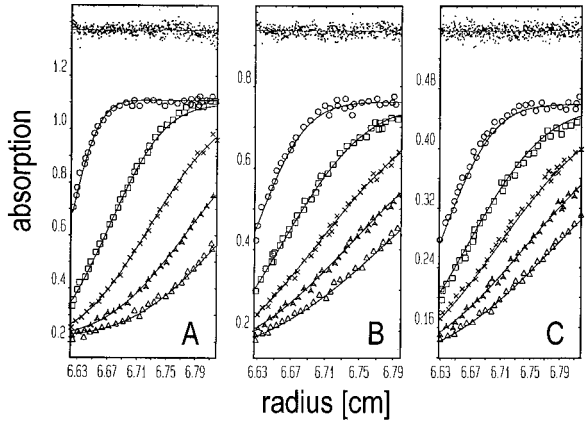

FIGURE 3: Radial concentration distribution (symbols) and fitted data (curves) of yeast hexokinase 2 as obtained from sedimentation velocity experiments. (A) Nonphosphorylated wild-type enzyme; (B) glutamate-14 hexokinase; (C) phosphoserine-14 enzyme. Solvent: 50 mM potassium phosphate buffer, pH 7.4, containing 1 mM PMSF, 1 mM EDTA, and 1 mM DTT. Loading enzyme concentration: 0.90 mg/mL (A), 0.60 mg/mL (B), and 0.33 mg/mL (C). Time interval between two scans: 18 min. Temperature: 20 °C. Residuals (above) are given in 4-fold (A, B) or 2-fold (C) amplification.

molecular mass of about 100 kDa (Table 3) which coincides within the limits of error with the result of equilibrium sedimentation (Table 2). In addition, a frictional ratio $f/f_0 = 1.29 \pm 0.02$ was calculated, indicating a shape of the protein deviating from that of a sphere. Similar results were obtained with the mutant enzymes carrying alanine, cysteine, and glutamate, respectively, at position 157 (Table 3). In contrast, substitution of serine-14 by glutamate gave a significantly different moving boundary pattern (Figure 3B) reflecting a drastic decrease of the sedimentation coefficient and corresponding to a molecular mass of 53.4 ± 1.0 kDa. The frictional ratio $f/f_0 = 1.22 \pm 0.02$ (Table 3) representing the dissociated form of the enzyme is indicative of a more sphere-like shape of this species. Sedimentation analysis of the *in vivo* phosphorylated enzyme (Figure 3C) resulted in hydrodynamic data which are indistinguishable from those obtained with the permanently pseudophosphorylated glutamate-14 hexokinase (Table 3). The hydrodynamic parameters determined for alanine-14 hexokinase (Table 3) confirm the molecular changes detected by equilibrium sedimentation (Table 2).

Kinetic Properties of Different Forms of Wild-Type and Mutant Hexokinases. Table 4 summarizes the basic kinetic parameters, V_{max} and K_M, of nonphosphorylated wild-type enzyme, phosphoserine-14 hexokinase, and mutant enzymes modified at position 14 as determined *in vitro* for glucose and MgATP. All the parameters calculated by nonlinear least-squares fitting correspond to final assay concentrations for hexokinase of 0.2−0.4 μg/mL. Under these experimental conditions, there is no significant difference in the glucose affinity or maximum rate to be observed as a consequence of serine-14 phosphorylation or substitution. For comparison, the kinetic data of serine-157 mutant hexokinases determined at enzyme concentrations of 1−5 μg/mL (*23*) are included.

Table 4: Effect of Substitution/Modification of Serine-14 and Serine-157, Respectively, on Yeast Hexokinase 2 Catalysis

Hxk2 species	rel V_{max}[b,c] (%)	K_M(Glc)[c] (μM)	K_M(ATP)[c] (μM)	V_{max}/K_M(Glc)[c]
Hxk2(S14/S157)[a]	100	160	140	0.59
Hxk2(S14A/S157)	100	160	140	0.62
Hxk2(S14E/S157)	105	155	150	0.68
Hxk2(S14p/S157)	97	180	130	0.54
Hxk2(S14/S157A)	5.3	28	460	0.19
Hxk2(S14/S157C)	1.4	57	470	0.024
Hxk2(S14/S157E)	—[d]	—[d]	—[d]	—[d]

[a] Wild-type enzyme carrying serine-14 and serine-157 unsubstituted/unmodified. [b] Average specific catalytic activity of purified nonphosphorylated wild-type hexokinase corresponding to a relative V_{max} of 100% was 380 units/mg. [c] Enzyme activity was measured with glucose as sugar substrate under standard assay conditions otherwise. Protein determination was according to Bradford (*50*). Nonlinear regression analysis assumed Michaelis−Menten kinetics. Deviations from the mean did not exceed 15%. [d] No activity detectable. The data of serine-157 mutant hexokinases are taken from (*23*).

DISCUSSION

Hexokinase is somehow involved in sugar sensing and in the establishment of glucose repression in *Saccharomyces cerevisiae* (e.g., *3*−*7*). Isoenzyme 2 has two functionally different phosphorylation sites (*21*, *23*) and can be a phosphoprotein *in vivo* (*20*), but neither a physiological role of phosphorylation at serine-14 nor the enzymes responsible in the cell are known. The aim of the present work was to explore the structural and functional consequences of hexokinase phosphorylation. For this purpose, different forms of wild-type hexokinase and mutant enzymes obtained by amino acid substitution at either site of specific phosphorylation were subjected to sedimentation and kinetic analysis. The consequences of permanent pseudophosphorylation as accomplished by serine−glutamate exchange introducing a phosphate-like negatively charged residue were compared for serine-14 to those resulting from phosphorylation *in vivo*. The basic finding of serine-14 phosphorylation or substitution by glutamate to cause enzyme dissociation (at least *in vitro*) and apparently without influencing the catalytic properties of the purified enzyme (Table 4) is in contrast to autophosphorylation at serine-157 which, though completely and reversibly inactivating hexokinase (*23*), does not affect the gross conformation and monomer−dimer equilibrium (Tables 2 and 3). The dissociative effect of pseudophosphorylation at the *in vivo* phosphorylation site suggests monomer formation to require the introduction of a negative charge rather than a phosphate-specific structure of the modifying group at this position.

The molecular details of hexokinase assembly and intersubunit interaction are still unknown. The mode of subunit interaction proposed by Colowick (*35*) to explain glucose stimulation of tryptic modification of the yeast hexokinases excludes direct contact of the two N-termini. Bennett and Steitz (*24*) suggested from X-ray data a nonsymmetrical subunit assembly for isoenzyme 2; however, their hypothetical dimer was modeled from an incomplete primary structure (*36*). Later sequence information (*27*, *28*) as well as the Edman degradation shows two pairs of basic amino acids before serine-14. These would be expected to counteract oligomeric stability if there were direct contact of the N-termini, phosphorylation in this region to promote monomer association rather than the opposite result observed here. Therefore, the dissociative effect of serine-14 phosphorylation might be a modification-induced conformational change

which impairs intersubunit interaction in part via a destruction of dipole contacts that could conceivably be formed by the two serine-14 hydroxyls to (so far unknown) residues of the neighboring monomer, respectively [in alanine-14 hexokinase, the energy of subunit interaction should be weakened by about 2 kcal/mol of monomer since substitution of methyl groups for serine residues should introduce weaker van der Waals forces and thereby contribute to the lower weight-average molecular mass determined by sedimentation analysis (Tables 2 and 3)].

According to the X-ray structure (*37*, *38*), monomeric hexokinase can be considered as a sphere-like molecule exhibiting slightly different radii. When fitting the molecule by an ellipsoid of revolution, an axial ratio of approximately 2 can be assumed which is in agreement with a frictional ratio of 1.2 as derived from hydrodynamic mobility (Table 3). The asymmetric assembly of two such polypeptide chains should give rise to the formation of a dimeric molecule with a significantly higher axial ratio. This expectation is verified by the higher frictional ratio of about 1.3 as obtained with dimeric hexokinase (Table 3). Even though the hydrodynamic data presented in this work fit the general rule of asymmetric assembly of dimeric proteins (*39*), the case for yeast hexokinase remains hypothetical without a three-dimensional structure which includes the N-terminus of the enzyme [the model by Bennett and Steitz (*24*) lacks the 20 N-terminal amino acids including the *in vivo* phosphorylation site of hexokinase].

Remarkably, substitution/modification of serine-157, which is known to be highly conserved and critically involved in determining the conformational state, hexose affinity, and catalytic activity of eukaryotic hexose kinases (*24*, *40*−*44*), turned out not to affect the oligomeric structure and the overall molecular shape of yeast isoenzyme 2 (Tables 2 and 3). This finding is in agreement with a location of serine-157 in a pocket harboring the active site (*24*), thus resulting in sterical exclusion of the respective residue at this position from direct participation in subunit interaction but still allowing the conformational changes which are necessarily involved in catalysis and activity regulation.

The similar catalytic properties of purified wild-type, mutant, and phosphohexokinases observed *in vitro* (Table 4) and the reversible autophosphorylation−inactivation (*23*) that can be correlated to the dimeric form of the enzyme (Tables 2 and 3) raise the question of the physiological significance of conversion of dimeric hexokinase into the monomeric form. Compared to enzyme dissociation forced by *in vitro* truncation removing at least 12 N-terminal amino acids (*17*−*19*), the single phosphorylation at serine-14 occurring *in vivo* turned out to be sufficient alone and is thus a potential mechanism for controlling the oligomeric state of hexokinase in the cell. Even though it is not yet known whether such a control has a physiological effect, earlier work showed that a monomeric form of hexokinase (the S-form enzyme; *16*, *45*) has a much lower K_M for glucose than the dimer. If that were also the case *in vivo*, then hexokinase dissociation caused by phosphorylation might accordingly compensate for the lower glucose concentration which initially stimulated enzyme modification. Since the standard assay conditions employ enzyme concentrations in the nanomolar range which likely favor enzyme dissociation (*15*, *16*, *19*), the similar kinetics obtained *in vitro* with phosphohexokinase and nonphosphorylated enzyme (Table 4) do not prove their functional equivalence in the cell, and work on the use of stopped flow and other techniques for this purpose is in progress.

Finally, one may also speculate on models of signal transduction where a direct nuclear role of hexokinase 2 in gene expression is influenced by its serine-14 phosphorylation and increased monomerization as stimulated by glucose limitation. Hexokinase 2 has been detected in the yeast nucleus (*46*, *47*) and has an N-terminal bipartite motif of basic residues (Lys^6-Lys^7-Pro-Gln-Ala-Arg^{11}-Lys^{12}) resembling a nuclear targeting sequence (*48*). Since the exclusion limit of nuclear pores is slightly higher than the molecular mass of monomeric hexokinase and/or enzyme dissociation might expose (*35*) the nuclear localization sequence, intranuclear hexokinase might affect transcriptional regulation of carbohydrate metabolism. A recent study which also presents data on the *in vivo* phosphorylation reports altered glucose repression in a *hxk2(S14A)* mutant strain (*49*).

REFERENCES

1. Gancedo, J. M., Clifton, D., and Fraenkel, D. G. (1977) *J. Biol. Chem. 252*, 4443−4444.
2. Herrero, P., Galindez, J., Ruiz, N., Martinez-Campa, C., and Moreno, F. (1995) *Yeast 11*, 137−144.
3. Entian, K.-D. (1980) *Mol. Gen. Genet. 178*, 633−637.
4. Ma, H., and Botstein, D. (1986) *Mol. Cell. Biol. 6*, 4046−4052.
5. Rose, M., Albig, W., and Entian, K.-D. (1991) *Eur. J. Biochem. 199*, 511−518.
6. Trumbly, R. J. (1992) *Mol. Microbiol. 6*, 15−21.
7. De Winde, J. H., Crauwels, M., Hohmann, S., Thevelein, J. M., and Winderickx, J. (1996) *Eur. J. Biochem. 241*, 633−643.
8. Lobo, Z., and Maitra, P. K. (1977) *Arch. Biochem. Biophys. 182*, 637−643.
9. Walsh, R. B., Clifton, D., Horak, J., and Fraenkel, D. G. (1991) *Genetics 128*, 521−527.
10. Hoggett, J. F., and Kellett, G. L. (1976) *Eur. J. Biochem. 66*, 65−77.
11. Schultze, I. T., and Colowick, S. P. (1969) *J. Biol. Chem. 244*, 2306−2316.
12. Easterby, J. S., and Rosemeyer, M. A. (1972) *Eur. J. Biochem. 28*, 241−252.
13. Derechin, M., Rustum, Y. M., and Barnard, E. A. (1972) *Biochemistry 11*, 1793−1797.
14. Shill, J. P., Peters, B. A., and Neet, K. E. (1974) *Biochemistry 13*, 3864−3871.
15. Furman, T. C., and Neet, K. E. (1983) *J. Biol. Chem. 258*, 4930−4936.
16. Womack, F., and Colowick, S. P. (1978) *Arch. Biochem. Biophys. 191*, 742−747.
17. Schmidt, J. J., and Colowick, S. P. (1973) *Arch. Biochem. Biophys. 158*, 458−470.
18. Schmidt, J. J., and Colowick, S. P. (1973) *Arch. Biochem. Biophys. 158*, 471−477.
19. Ma, H., Bloom, L. M., Dakin, S. E., Walsh, C. T., and Botstein, D. (1989) *Proteins: Struct., Funct., Genet. 5*, 218−223.
20. Vojtek, A. B., and Fraenkel, D. G. (1990) *Eur. J. Biochem. 190*, 371−375.
21. Kriegel, T. M., Rush, J., Vojtek, A. B., Clifton, D., and Fraenkel, D. G. (1994) *Biochemistry 33*, 148−152.
22. Fernandez, R., Herrero, P., Fernandez, E., Fernandez, T., Lopez-Boado, Y. S., and Moreno, F. (1988) *J. Gen. Microbiol. 134*, 2493−2498.
23. Heidrich, K., Otto, A., Behlke, J., Rush, J., Wenzel, K.-W., and Kriegel, T. (1997) *Biochemistry 36*, 1960−1964.
24. Bennett, W. S., Jr., and Steitz, T. A. (1980) *J. Mol. Biol. 140*, 183−230.

25. Fernandez, R., Herrero, P., Gascon, S., and Moreno, F. (1984) *Arch. Microbiol. 139*, 139−142.
26. Meltzer, N. M., Tous, G. I., Gruber, S., and Stein, S. (1987) *Anal. Biochem. 160*, 356−361.
27. Fröhlich, K.-U., Entian, K.-D., and Mecke, D. (1985) *Gene 36*, 105−111.
28. Stachelek, C., Stachelek, J., Swan, J., Botstein, D., and Konigsberg, W. (1986) *Nucleic Acids Res. 14*, 945−963.
29. Cohn, E. J., and Edsall, J. T. (1943) in *Proteins, amino acids and peptides*, Academic Press, New York.
30. Ansevin, A. T., Roark, D. E., and Yphantis, D. A. (1970) *Anal. Biochem. 34*, 237−261.
31. Yphantis, D. A. (1964) *Biochemistry 3*, 297−317.
32. Behlke, J., Ristau, O., and Schönfeld, H.-J. (1997) *Biochemistry 36*, 5149−5156.
33. Behlke, J., and Ristau, O. (1997) *Biophys. J. 72*, 428−434.
34. Pessen, H., and Kumosinski, T. F. (1985) *Methods Enzymol. 117*, 219−255.
35. Colowick, S. P. (1973) in *The Enzymes* (Boyer, P. D., Ed.) Vol. 6, pp 1−48, Academic Press, New York.
36. Harrison, R. W. (1985) Ph.D. Thesis, Yale University, New Haven, CT.
37. Bernstein, F. C., Koetzle, T. F., Williams, G. J. B., Meyer, E. E., Jr., Brice, M. D., Rodgers, J. R., Kennard, D., Shimanuchi, T., and Tasumi, M. (1977) *J. Mol. Biol. 112*, 535−542.
38. Anderson, C. M., Steenkamp, R. E., and Steitz, T. A. (1978) *J. Mol. Biol. 123*, 15−23.
39. Haschemeyer, R. H., and Bowers, W. H. (1970) *Biochemistry 9*, 435−445.
40. Schirch, D. M., and Wilson, J. E. (1987) *Arch. Biochem. Biophys. 257*, 1−12.
41. Andreone, T. L., Printz, R. L., Pilkis, S. J., Magnuson, M. A., and Granner, D. K. (1989) *J. Biol. Chem. 264*, 363−369.
42. Arora, K. K., Filburn, C. R., and Pedersen, P. L. (1991) *J. Biol. Chem. 266*, 5359−5362.
43. Xu, L. Z., Zhang, W., Weber, I. T., Harrison, R. W., and Pilkis, S. J. (1994) *J. Biol. Chem. 69*, 27458−27465.
44. Xu, L. Z., Weber, I. T., Harrison, R. W., Gidh-Jain, M., and Pilkis, S. J. (1995) *Biochemistry 34*, 6083−6092.
45. Mayes, E. L., Hoggett, J. G., and Kellett, G. L. (1983) *Eur. J. Biochem. 133*, 127−134.
46. Van Tuinen, E., and Riezman, H. (1987) *J. Histochem. Cytochem. 35*, 327−333.
47. Randez-Gil, F., Herrero, P., Sanz, P., Prieto, J. A., and Moreno, F. (1998) *FEBS Lett. 425*, 475−478.
48. Dingwall, C., and Laskey, R. A. (1991) *Trends Biochem. Sci. 16*, 478−481.
49. Randez-Gil, F., Sanz, P., Entian, K.-D., and Prieto, J. A. (1998) *Mol. Cell. Biol. 18*, 2940−2948.
50. Bradford, M. M. (1976) *Anal. Biochem. 72*, 248−254.

BI980914M